Flow balancing in extrusion dies for thermoplastic profiles: non-isothermal effects

J. M. Nóbrega (1), O. S. Carneiro(1), P. J. Oliveira (2), F. T. Pinho (3)
(1)Department of Polymer Engineering, Universidade do Minho, Campus de Azurém, 4800-058 Guimarães, Portugal
(2)Departamento de Engenharia Electromecânica, Universidade da Beira Interior, Rua Marquês D'Ávila e Bolama, 6200 Covilhã, Portugal
(3)Centro de Estudos de Fenómenos de Transporte, DEMEGI, Faculdade de Engenharia da Universidade do Porto, Rua Roberto Frias, 4200-465 Porto, Portugal

Abstract

In this work a methodology for the automatic balance of the flow in profile extrusion dies is improved and tested. The referred methodology encompasses a 3D computational code, based in the finite volumes method, to perform the numerical non-isothermal flow computations. The influence of some operating parameters (throughput, melt inlet temperature and flow channel wall temperature) and the effect of neglecting heat viscous dissipation is assessed. It was concluded that the throughput and increase in temperature due to viscous dissipation have negligible influence on the flow distribution. The other parameters (melt inlet temperature and wall temperature) proved to have some effect on the flow distribution, essentially depending on the area available for heat exchange with the outer wall of the flow channel. For the case study used in this work it was possible to reach a good final solution without any user intervention.

Introduction

In the past, the design of profile extrusion dies was based on experimental trial-and-error procedures, that rely heavily on the designers experience and are usually very time, material and equipment consuming [1]. Currently, due to the development of software packages for the mathematical modelling of the flow of polymer melts [2-6] this trial-and-error procedure is being progressively transformed from experimental to numerical. However, the generation of the successive solutions, and the decisions involved in this process, are still committed to the designer [1]. Furthermore, only recently some relevant post-extrusion phenomena were included in the models. For example, in the particular case of post-extrusion swelling it is already possible to automatically define the contour of the final zone of the extrusion die (parallel zone) [7,8], but the first trial for the geometry of the extrusion head must be completely defined by the user and the automatic procedure only acts on the final parallel zone of the die. Anyway, the automatic design of profile extrusion dies is still incipient, since it ignores, amongst other things, the need for balancing the flow along the die exit contour. To match these objectives, especially for complex geometries, the flow should be ideally modelled in 3D [9]. However, this is usually not very attractive to designers since it requires unacceptable turnaround times for results, mainly due to the time required for calculation and for geometry and grid generation [9].
This work is a contribution towards the 'Automatic Extrusion Die Design' concept and it includes developments into an existing computational code [10] based on the finite volume method, namely the introduction of the energy equation for non-isothermal calculations. This option was induced by recent research efforts into 3D problems, which have shown that the modelling based on the finite volumes

method should help to reduce the time required for calculation [11]. A routine for the automatic definition of the geometry was also developed. This will be used as input to the existing pre-processor of the computational rheology code, which generates the computational grid required for the numerical flow simulations. This routine allows the use of non-uniform, non-orthogonal grids mapping the flow area in order to predict complex flows and reduce computational requirements. The developed routine, the pre-processor and the computational code were integrated smoothly as part of the whole die design code.
In the first part of this work, the general methodology used to balance the flow in a profile extrusion die is described. The performance of the automatically generated die geometries is evaluated through an objective function that takes into account the flow balancing [1,12] and the ratio L/t of the parallel zone. The numerical calculations of the three-dimensional, non-isothermal flow are performed assuming a generalized Newtonian fluid constitutive equation with a Bird Carreau viscosity model and an Arrhenius-type temperature dependence.
In the second part of the work, the influence of the operating parameters throughput, melt inlet temperature and die surface temperature on the flow balance is assessed. The influence of viscous dissipation is also investigated.
As a result, this work will help to select the most relevant factors to be considered in the automatic design of the flow channel of profile extrusion dies, as part of a global optimisation die design algorithm.

Methodology

The first task to be considered in the die design procedure is the flow balance [12,13] in which the flow channel is divided into four main geometrical zones [13], namely the die land or parallel zone (PZ), the pre-parallel zone (PPZ), the transition zone (TZ) and the adapter (A), all shown in Figure 1. The cross section of the parallel and the pre-parallel zones is divided into elemental sections (ES) [13], shown in Figure 2, which have independent controllable length with constant thickness (L_i). For flow balance purposes it will be sufficient to model the flow in the pre-parallel and parallel zones of the die (PPZ+PZ), since the two final sections of the die dominate the flow distribution [9,13,14].

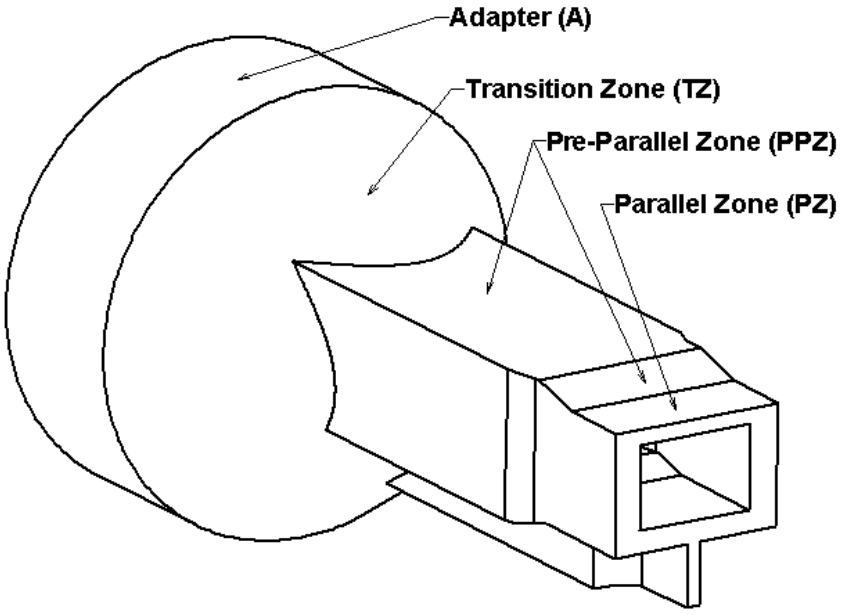

Figure 1 - Flow channel of a profile extrusion die split in its main geometrical zones.

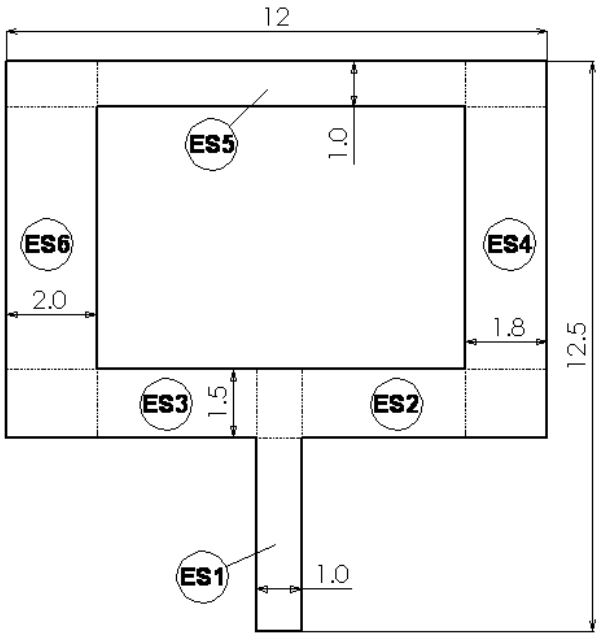

Figure 2 - Cross section of the parallel zone (PZ) and elemental sections (ES) considered (dimensions in mm).

The objective of the algorithm is to find the set of lengths (L_i) that results in the most balanced geometry. The maximum and minimum admissible values for the ratio length/thickness (L/t) were considered to be 15 and 1, respectively. As stated in the literature L/t values below 7 are not advisable [15]. However, it would not be wise to reject a trial geometry perfectly balanced having an L/t slightly lower than 7, since the limit values are purely empirical, resulting from industrial practice. Therefore, in this work the quality of each trial geometry is assessed by an objective function (F_{obj}), which combines two criteria affected by different weights: flow balance and ratio L/t:

$$F_{obj} = \sum_{i=1}^{4} \left\{ \alpha \left(1 - \frac{V_i}{V_{av}} \right)^2 + k(1-\alpha) \left[1 - \frac{(L/t)_i}{(L/t)_{opt}} \right]^2 \right\} \quad (1)$$

with $k = 0$ for $(L/t)_i \geq (L/t)_{opt}$ and $k = 1$ for $(L/t)_i < (L/t)_{opt}$

where:

V_{av}, V_i - average velocities of the extrudate and of the flow in each ES, respectively
$(L/t)_i$ - ratio between length and thickness of each ES
$(L/t)_{opt}$ - optimum value for the ratio L/t (considered to be 7)
α - relative weight (considering the higher relative importance of the flow balance criterion, α was considered to be 0.75)

The value of the objective function decreases with increasing performance of the die, being zero for a balanced die with all the ES lengths in the admissible range.

The flow balance methodology tested here is based on a previous method developed in [13,14] with two additional improvements:

1) The search process used to find the best geometry is based on the value of the objective function;
2) The process starts with coarse meshes and progressively performs mesh refinements as the final solution is approached.

Outline of the numerical procedure

The calculation of the flow field is performed by a self-contained part of the code that has been developed for the computation of isothermal viscoelastic flows and is described and tested in detail in a series of papers [10,16,17]. Here, we just give a quick overview of the calculation procedure, which solves a set of equations for fluid flow, and which has been here extended to account also for the solution of the energy equation.
The basic equations to be solved are those expressing conservation of mass

$$\frac{\partial u_j}{\partial x_j} = 0 \tag{2}$$

of linear momentum

$$\frac{\partial \rho u_i}{\partial t} + \frac{\partial \rho u_j u_i}{\partial x_j} = -\frac{\partial p}{\partial x_i} + \frac{\partial \tau_{ij}}{\partial x_j} \tag{3}$$

of energy

$$\frac{\partial \rho c T}{\partial t} + \frac{\partial \rho c u_i T}{\partial x_i} = \frac{\partial}{\partial x_i}\left(\frac{\partial k T}{\partial x_i}\right) + \tau_{ij}\frac{\partial u_i}{\partial x_j} \tag{4}$$

and a constitutive rheological equation for the stress field τ_{ij}. In these equations u_i is the velocity component in a Cartesian co-ordinate frame, ρ is the fluid density, p is an isotropic pressure, T is the temperature, k is the thermal conductivity and c is the specific heat. The last term of the RHS of equation 3 accounts for the viscous dissipation. In the present computations the generalised Newtonian rheological constitutive equation was considered

$$\tau_{ij} = \eta(\dot{\gamma}, T)\left(\frac{\partial u_i}{\partial x_j} + \frac{\partial u_j}{\partial x_i}\right) - \frac{2}{3}\eta(\dot{\gamma}, T)\frac{\partial u_k}{\partial x_k}\delta_{ij} \tag{5}$$

where η is the dynamic viscosity of the fluid. The velocity divergence in the last term of equation 5 vanishes for incompressible flows, but is kept in the code for stability reasons. The dynamic viscosity is a function of the second invariant of the rate of deformation tensor $\dot{\gamma} \equiv \sqrt{2\,\mathrm{tr}D^2}$ where

$$D_{ij} = \frac{1}{2}\left(\frac{\partial u_i}{\partial x_j} + \frac{\partial u_j}{\partial x_i}\right) \tag{6}$$

and of temperature. In this paper, the adopted viscosity model was $\eta(\dot{\gamma}, T) = F(\dot{\gamma})H(T)$. The shear rate dependence contribution was given by the Bird-Carreau equation [18]

$$F(\dot{\gamma}) = \eta_\infty + \frac{\eta_0 - \eta_\infty}{\left(1 + (\lambda\dot{\gamma})^2\right)^{\frac{1-n}{2}}} \tag{7}$$

where η_∞ is the infinite-shear-rate viscosity, η_0 is the zero-shear-rate viscosity, λ is a time constant (i.e., the inverse of the shear-rate at which the fluid changes from Newtonian to power-law behaviour) and *n* is power-law index. The Arrhenius law was used to account for the viscosity temperature dependence:

$$H(T) = \exp\left[\alpha\left(\frac{1}{T} - \frac{1}{T_\alpha}\right)\right] \tag{8}$$

where α is the ratio of the activation energy to the perfect gas constant and T_α is the reference temperature (in Kelvin) for which $H(T) = 1$.

Given the similarity of the energy and linear momentum equations, the discretization and numerical solution of the energy equation is akin to that of the linear momentum provided u_i is substituted by T and the coefficients of the equations are modified in accordance with the original conservation equations. The numerical solution of the energy equation was inserted into the sequential algorithm so that it is the last equation of the set to be solved in each iteration, as it assumes knowledge of the flow field.

Three-dimensional grids were required for these simulations and they had to be sufficiently fine to capture the main flow characteristics and to show the feasibility of the methodology. The most refined mesh used was 10 cells thick in any of its elemental sections (ES). Figure 3 shows a typical mesh used in the calculations with the geometry depicted in Figures 1 and 2.

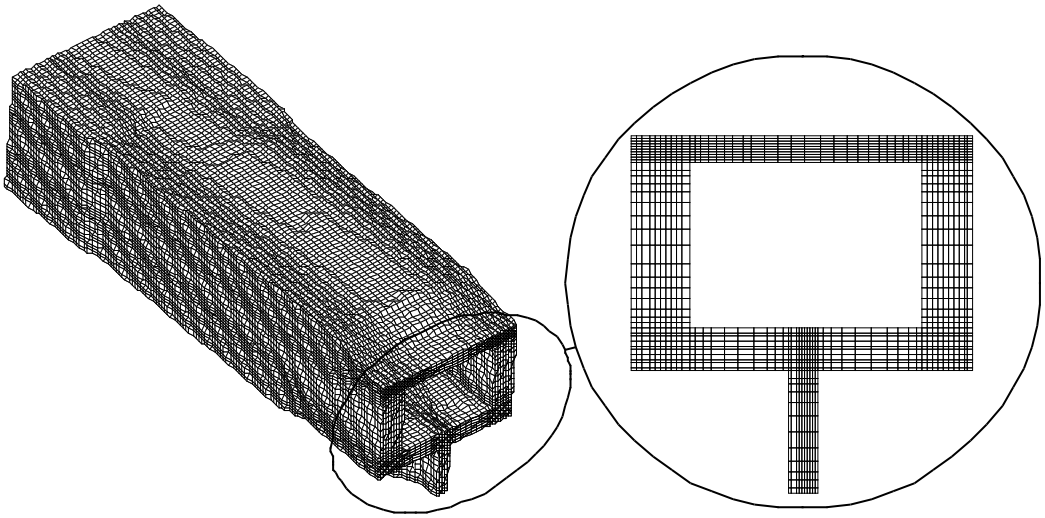

Figure 3 – Typical mesh used in the calculations.

Case Study

The polymer used in the simulations was a polypropylene homopolymer extrusion grade, Novolen PPH 2150, from Targor. Its rheological behaviour was experimentally characterised by capillary and rotational reometers, at 210ºC, 230ºC and 250ºC. The shear viscosity was least-squared fitted by a Bird-Carreau constitutive equation combined with the Arrhenius law (equations 7 and 8), that produced the following parameters: η_∞(Pa.s)=0, η_0(Pa.s)=5.58x10^4, λ(s)=3.21, n=0.3014, α(ºC)= 2.9 x10^3 and T_0(ºC)=230.
The flow balance methodology was used to design the flow channel of the extrusion die shown in Figure 1, adopting the division in elemental sections (ES) illustrated in Figure 2.
The cross section of the flow channel had sections of different thickness (shown in Figure 2), in order to enforce an unbalanced geometry.
The conditions used in the calculations are defined in Table 1.

Table 1 – Operating conditions

Flow rate*	16.5 kg/h
Melt inlet temperature	230 ºC
Outer die walls temperature	230 ºC
Inner (mandrel) die walls	Insulated

* Corresponding to an average velocity of 100 mm/s at the die exit

As stated above the simulations of the flow were only performed in the die zones relevant for this purpose, i.e., PPZ and PZ. In a previous work [19] it was concluded that the parameter that most influences the flow balance is the length of (PPZ+PZ) having a constant thickness (L). As a consequence, the other dimensions of the PPZ, defined in Figure 4, were fixed (entrance thickness of 3 mm and convergence angle (α) of 30º for all the ES), i.e., only the lengths L_i of each ES needed to be determined.

At the beginning of the calculations the ratio L/t for all ES was considered to be 15.0, and the computational mesh was coarse representing the ES with 2 cells only.

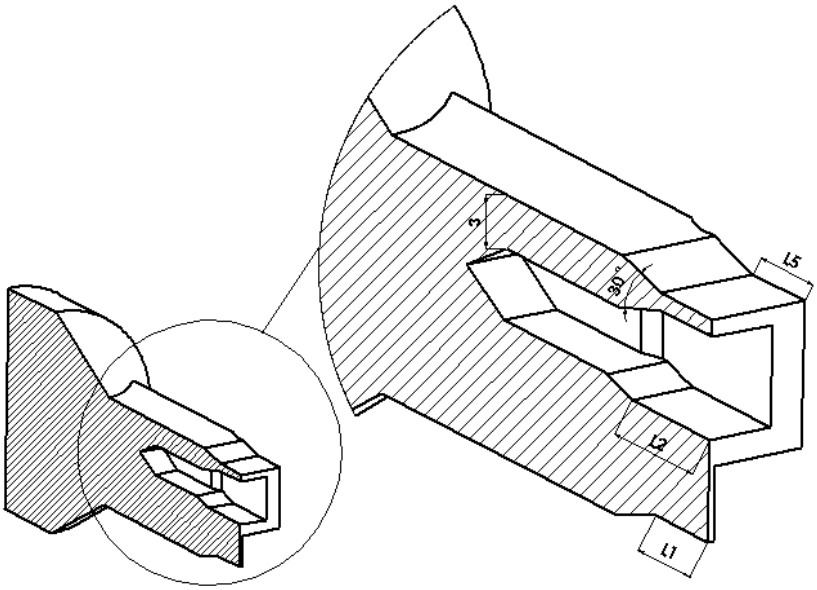

Figure 4 – Side view cut of the flow channel illustrating the constructive solution adopted and showing some relevant dimensions (mm).

A typical grid used in the final stages of the calculations, with 10 cells along the thickness (a total of 162,840 cells for the whole geometry), is shown in Figure 3. The typical calculation time required for each iteration of the optimisation code using this mesh, including the time required for grid generation and flow field calculation, is 2 hours using a Pentium III computer running at 933MHz.

Results and discussion

Performance of the methodology

The results obtained through the use of the flow balance methodology are illustrated in terms of the variations of the objective function, the ratio L/t and the average velocity ratio in Figures 5(a), (b) and (c), respectively. As expected, in the first iteration there are significant differences in the average velocities as a consequence of the previously mentioned cross section unbalance. The improvement obtained in terms of velocity distribution is shown in the contours of Figure 6. The best solution is attained at iteration 11 for which the average velocities in all but ES6 are within 10% of the global bulk velocity. At ES6 the difference is 20% because the relative flow restriction is very low. A possible solution would be the inclusion of a local flow separator, to isolate the section [13].

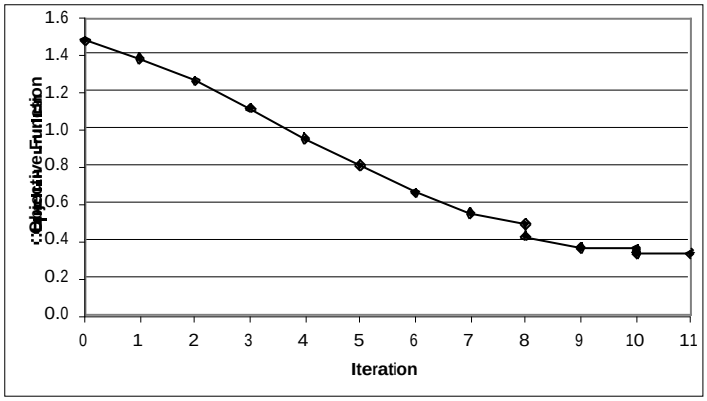

(a)

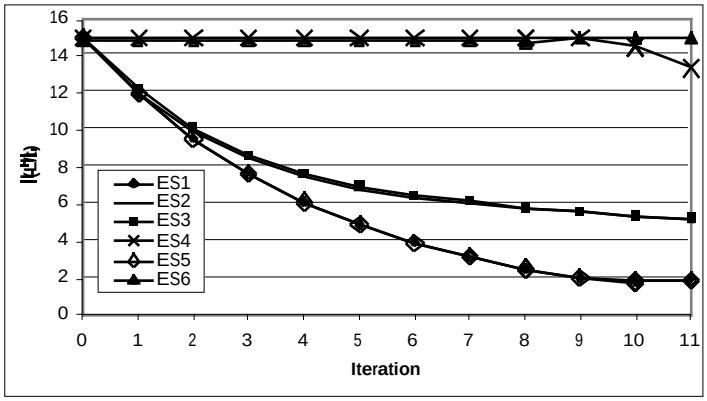

(b)

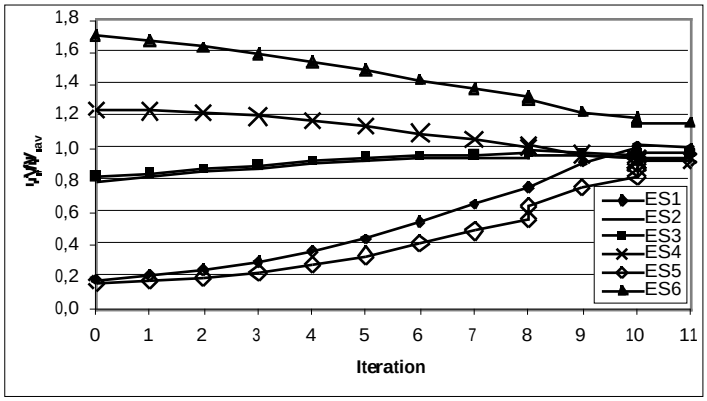

(c)

Figure 5 - Results of simulations performed in successive iterations: (a) objective function; (b) ratio length/thickness of the parallel zone of each elemental section; (c) relative average velocity in each elemental section. Note: the discontinuities observed in the curves correspond to iterations at which the mesh was refined.

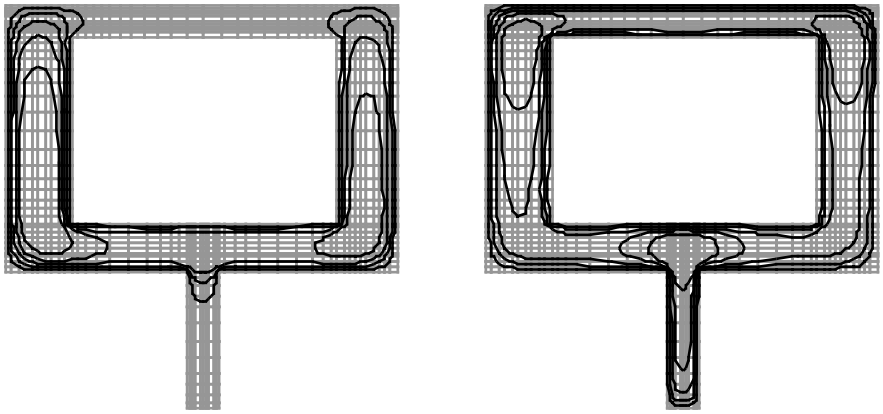

(a) (b)

Figure 6 - Contours of the axial velocity computed for: (a) initial trial geometry; (b) best result obtained by the methodology.

The variation of the calculation time with mesh refinement and the difference between the length of each elemental section relative to their final values are shown in Figure 7. It is worth mentioning that after 1 hour of calculation all the ES lengths differ by less than 10% from their final values. Hence, the flow distribution is shown to be almost insensitive to meshes that have more than 4 elements along the thickness and, in this case, the last 30 hours of calculations were mainly useful for assessment purposes. Naturally, they are needed if more accuracy on the absolute values of the velocity and temperature distribution is required.

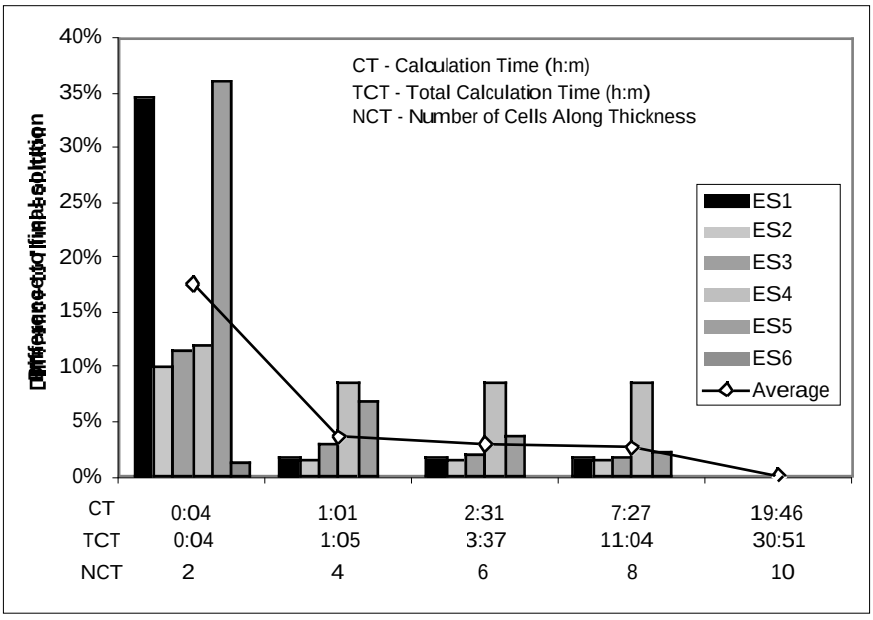

Figure 7 – Progress of the results (in terms of length) at the end of each mesh refinement stage.

Influence of process parameters

The influence of the inlet temperature, flow channel wall temperature and throughput (die exit average velocity) on flow balance is shown in Figure 8.

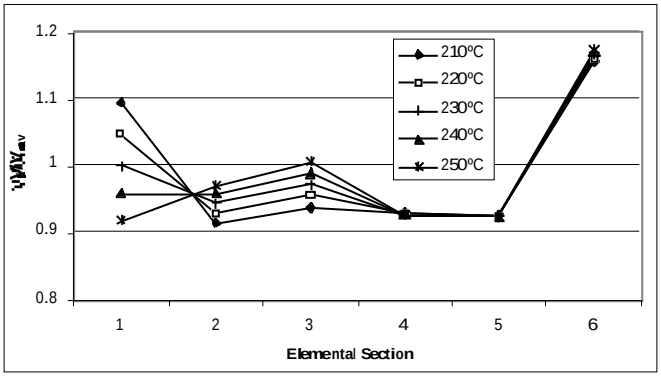

(a)

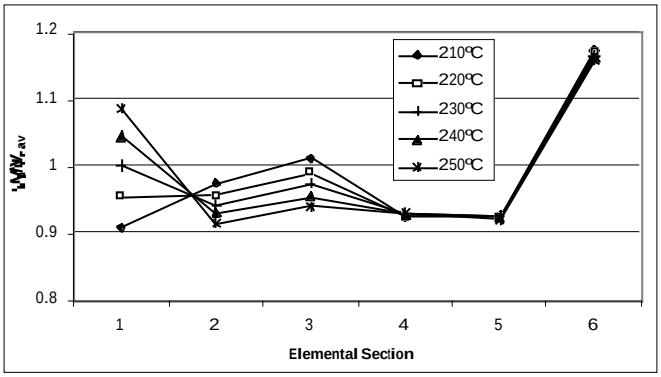

(b)

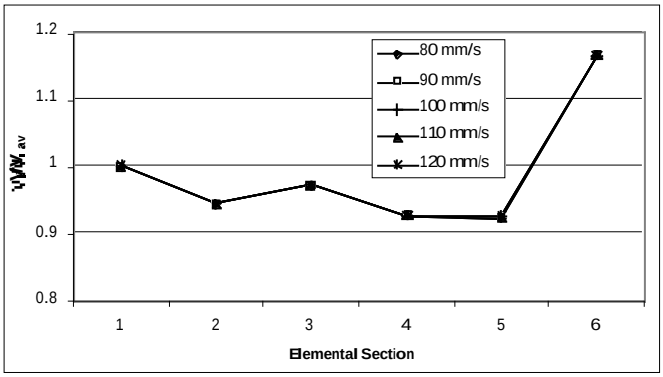

(c)

Figure 8 – Influence of some operating parameters in the flow distribution: (a) melt inlet temperature; (b) channel wall temperature; (c) throughput (die exit average velocity).

As can be observed, the flow distribution is not very sensitive to the variations imposed. The most sensitive elemental section is ES1, showing a maximum variation of circa ± 10% in the average velocity when varying the temperature parameters. This is a consequence of its low thickness and high relative

area for heat exchange with the outer wall. In order to compensate for that variation, the neighbouring elemental sections (ES2 and ES3) are also affected.

In Figure 9 the effect of viscous dissipation is shown. It can be concluded that, for this case study, viscous dissipation has almost no influence on the flow distribution. This result is not surprising since the maximum temperature rise promoted by viscous dissipation was determined to be circa 7 ºC. However the inclusion of non-isothermal effects is still important in order to check for the existence of hotspots due to excessive local viscous dissipation. Furthermore, it influences other aspects of the die performance, namely pressure drop and stresses developed, which are not being considered in this particular work. It should also be referred that the inclusion of the non-isothermal behaviour does not substantially affect the calculation time.

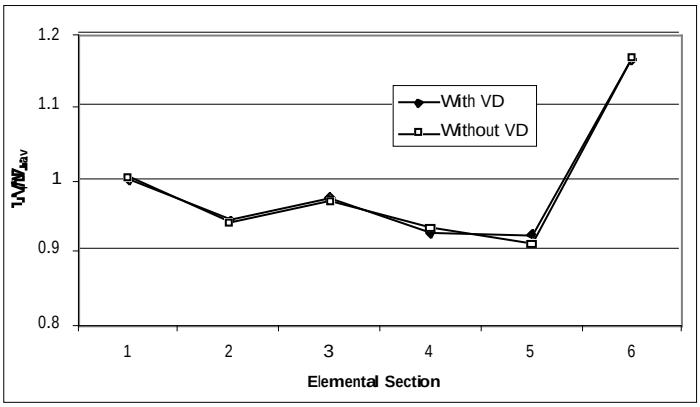

Figure 9 – Influence of viscous dissipation on flow distribution.

Conclusion

The automatic die design methodology used in this work has shown great potential since it performed well and quickly in a complex profile geometry, without any user intervention during the search/optimisation procedure.

The three-dimensional computational code developed for the numerical simulation of the flow by [10,16,17] was here successfully extended to account for non-isothermal flow. When coupled with the developed progressive mesh refinement technique, it resulted in a reasonable solution of the problem in just 1 hour of calculation.

The effect of some process parameters on flow distribution was assessed in this work. The flow distribution was found to be essentially affected by the melt inlet temperature and the flow channel wall temperature in regions of low thickness, and neighbouring sections, whereas throughput and viscous dissipation had negligible effects. However, note that flow distribution is assessed via a relative parameter, but in terms of absolute quantities these process parameters have a non-negligible effect. It is thus advisable to perform accurate non-isothermal calculations in order to account, amongst other things, for the possible existence of hotspots.

References

1. I. Szarvasy, J. Sienz, J. F. T. Pitman, E. Hinton, *Intern. Polym. Processing*, XV, 1, 28-39 (2000)
2. Polyflow, Fluent Inc.
3. Diecalc, Rapra Technology Ltd.
4. G. Menges, M. Kalwa, J. Schmidt, *Kunstst.*, 77, 8, 797-802 (1987)
5. J. Vlachopoulos, P. Behncke, J. Vlcek, *Adv. Polym. Tech.*, 9, 2, 147-156 (1989)
6. D. H. Sebastian, R. Rakos, *Adv. Polym. Tech.*, 5, 333-339 (1985)
7. H. -P. Wang, *Plastics Technology*, 42, 2, 46-49 (1996)
8. V. Legat, J. M. Marchal, *Int. J. Num. Methods Fluids*, 16, 29-41 (1993)
9. J. Svabik, L. Placek, P. Saha, *Intern. Polym. Processing*, XIV, 3, 247-253 (1999)
10. P. J. Oliveira, F. T. Pinho, G. A. Pinto, *J. Non-Newt. Fluid Mech.*, 79, 1-43 (1998)
11. S.-C. Xue, N. Phan-Thien, and R.I. Tanner, *J. Non-Newt. Fluid Mech.* 74, 195-245 (1998)
12. M. P. Reddy, E. G. Schaub,, L. G. Reifschneider, H. L. Thomas, *SPE Annual Technical Conference* (1999)
13. O. S. Carneiro, J. M. Nóbrega, F. T. Pinho, P. J. Oliveira, Computer Aided Rheological Design of Extrusion Dies for Profiles, *J. Mat. Processing Tech., in press*
14. J. M. Nóbrega, O. S. Carneiro, F. T. Pinho, P. J. Oliveira, *SPE Annual Technical Conference* (2001)
15. W. Michaeli, Extrusion Dies for Plastic and Rubber, Hanser Pub. (1992)
16. P. J. Oliveira, F. T. Pinho, *Num. Heat Transfer, Part B*, 35, 3, 295-315 (1999)
17. P. J. Oliveira, F. T. Pinho, *J. Non.Newt. Fluid Mech.*, 88, 63-88 (1999)
18. D. G. Baird, D. I. Collias, Polymer Processing – Principles and Design, Butterworth-Heinemann (1995), Chapter 2, pg 11
19. J. M. Nóbrega, O. S. Carneiro, F. T. Pinho, P. J. Oliveira, *2nd National Meeting of the Portuguese Society of Rheology* (2000)